ADVANCED HEALTHCARE MATERIALS
www.advhealthmat.de

Organic Photo-Electrochemical Transistor-Based Biosensor: A Proof-of-Concept Study toward Highly Sensitive DNA Detection

Jiajun Song, Peng Lin, Yi-Fan Ruan, Wei-Wei Zhao,* Weiwei Wei, Jin Hu, Shanming Ke, Xierong Zeng, Jing-Juan Xu, Hong-Yuan Chen, Wei Ren, and Feng Yan**

Organic bioelectronics have shown promising applications for various sensing purposes due to their significant advantages in term of high flexibility, portability, easy fabrication, and biocompatibility. Here, a new type of organic device, organic photo-electrochemical transistor (OPECT), is reported, which is the combination of an organic electrochemical transistor and a photo-electrochemical gate electrode modified with CdS quantum dots (QDs). Thanks to the inherent amplification function of the transistor, the OPECT-based biosensor exhibits much higher sensitivity than that of a traditional biosensor. The sensing mechanism of the OPECT is attributed to the charge transfer between the photosensitive semiconductor CdS QDs and the gate electrode. In an OPECT-based DNA sensor, target DNA is labeled with Au nanoparticles (NPs) and captured on the gate electrode, which can influence the charge transfer on the gate caused by the exciton–plasmon interactions between CdS QDs and Au NPs. Consequently, a highly sensitive and selective DNA sensor with a detection limit of around 1×10^{-15} M is realized. It is expected that OPECTs can be developed as a high-performance platform for numerous biological detections in the future.

Biosensors have attracted considerable research interest due to their important applications in disease diagnosis, medicine research, food safety, and environmental monitoring.[1–3] Enormous efforts among the community have been devoted to developing innovative biosensors with advanced properties such as rapid response and high sensitivity.[4–7] Over the past years, organic electrochemical transistors (OECTs) have been widely investigated for different biosensing applications, such as enzymatic sensing,[8,9] DNA detection,[10] immunoassay,[11] and cell-based analysis,[12,13] due to their desirable advantages including high sensitivity, low cost, low working voltage (<1 V), mechanical flexibility, and biocompatibility.[14,15] Moreover, microsized OECT arrays have been successfully prepared by special photolithography technique, making it possible to use OECTs for micro and high-throughput bioanalysis.[16,17]

Photo-electrochemical (PEC) bioanalysis is a newly emerged biomolecular detection technique that has promptly become a subject of hot research interest due to its attractive potential in future bioassays.[18–20] In a typical PEC system, light is utilized to excite photosensitive species on the working electrode, which would lead to charge transfer and thus a photocurrent as an electrical detection signal. The photocurrent is sensitive to a biorecognition event when it has interactions with the photosensitive species on the electrode, resulting in the operation of a PEC-based biosensor.[21] Due to the use of two separate signals for optical excitation and electrical detection, PEC bioanalysis has reduced background

J. J. Song, Dr. P. Lin, Dr. W. W. Wei, J. Hu, Dr. S. M. Ke, Prof. X. R. Zeng
Shenzhen Key Laboratory of Special Functional Materials & Guangdong Research Center for Interfacial Engineering of Functional Materials
College of Materials Science and Engineering
Shenzhen University
Shenzhen 518060, China
E-mail: lin.peng@szu.edu.cn

Y.-F. Ruan, Dr. W.-W. Zhao, Prof. J.-J. Xu, Prof. H.-Y. Chen
State Key Laboratory of Analytical Chemistry for Life Sciences and Collaborative Innovation
School of Chemistry and Chemical Engineering
Nanjing University
Nanjing 210093, China
E-mail: zww@nju.edu.cn

The ORCID identification number(s) for the author(s) of this article can be found under https://doi.org/10.1002/adhm.201800536.

DOI: 10.1002/adhm.201800536

Prof. W. Ren
Electronic Materials Research Laboratory
Key Laboratory of the Ministry of Education & International Center for Dielectric Research
Xi'an Jiaotong University
Xi'an 710049, China

Prof. F. Yan
Department of Applied Physics
The Hong Kong Polytechnic University
Hong Kong, China
E-mail: apafyan@polyu.edu.hk

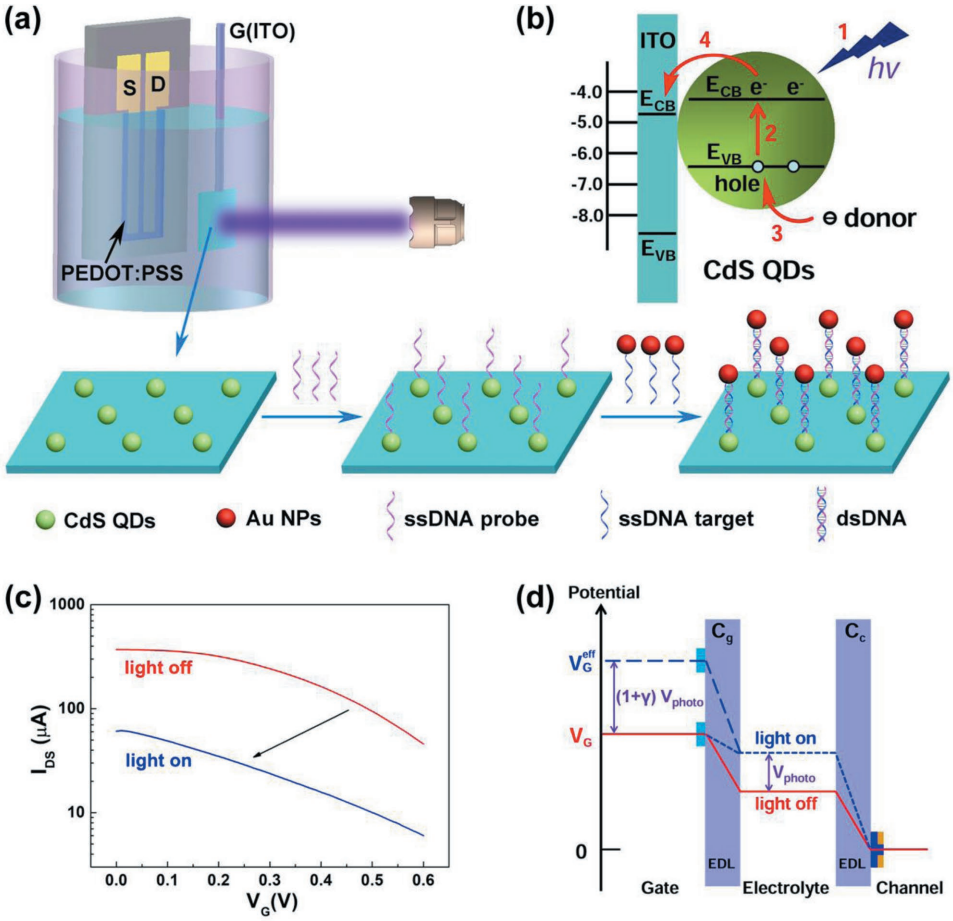

Figure 1. a) Schematic of an OPECT-based biosensor. b) Schematic of the charge transfer between CdS QDs and ITO gate electrode. c) Transfer characteristics (I_{DS} ~V_G, V_{DS} = 0.1 V) of an OPECT measured in AA solution before and after the light irradiation. d) The modulation of gate voltage applied on an OPECT due to the photovoltage V_{photo} induced by the light irradiation.

noise and thus possesses high sensitivity and low detection limit.[22,23] Recently, PEC biosensors have demonstrated considerable progress in enzymatic analysis,[24,25] immunoassay,[26,27] and DNA sensing.[28,29]

In this paper, considering that charge transfer on the gate electrode of an OECT can lead to the change of the effective gate voltage and thus the response of the channel current,[30] we integrate a PEC active gate electrode in an OECT to achieve a novel organic photo-electrochemical transistor (OPECT) and use it as a DNA sensor. Thanks to the amplification function of the transistor, the OPECT-based sensor demonstrates much higher sensitivity than that of traditional PEC bioanalysis. The device can detect the concentration of target DNA down to 1×10^{-15} M with good selectivity, which paves a way for ultrasensitive nucleic acid detection.[31]

Figure 1a shows the device design of an OPECT. Specifically, poly(3,4-ethylenedioxythiophene):poly(styrene sulfonate) (PEDOT:PSS) is used as the active layer of the device, indium tin oxide (ITO) glass modified with CdS quantum dots (QDs) is employed as the gate electrode and phosphate-buffered saline (PBS) solution containing 0.1 M ascorbic acid (AA) is used as the electrolyte. Under 420 nm light illumination (intensity: 0.2 mW cm^{-2}), CdS QDs absorb photons with energies higher than that of its bandgap, resulting in the excitation of electrons from the valence band (VB) to the conduction band (CB) and thus the formation of electron–hole pairs. As AA is a strong electron donor, the recombination of electron–hole pairs is effectively inhibited, leading to the stable transfer of the CB electrons to the ITO gate, as shown in Figure 1b.

Figure 1c shows the transfer curves (I_{DS} ~V_G, V_{DS} = 0.1 V) of an OPECT device measured before and after the light irradiation. It can be found that the transfer curve shifts significantly to lower gate voltage under the irradiation of light, which can be attributed to the increase of the effective gate voltage of the transistor. The sensing behavior of the OPECT is quite similar to that of a previously reported OECT sensitive to H_2O_2.[30]

The sensing mechanism of the OPECT is presented in Figure 1d. Since the electrolyte is conductive, the gate voltage is actually applied on the two interfaces in the OPECT, including gate/electrolyte and electrolyte/channel (organic semiconductor) interfaces.[32,33] Each interface has an electric double layer (EDL) that can be regarded as a capacitor. So the two EDLs on the gate and channel have the capacitances of C_g and C_c, respectively, which are connected in series in the device. Without light illumination, the potential drop at the

electrolyte/channel interface is $\frac{V_G}{1+\gamma}$, where $\gamma = C_c/C_g$.[30] Under light illumination, the electron transfer from the CB of CdS QDs to the ITO gate electrode can lead to the decrease of the potential drop at the gate/electrolyte interface. Assuming the changed value of the potential drop at the gate/electrolyte interface caused by the light irradiation is V_{photo}, the potential drop at the electrolyte/channel interface is increased to $\frac{V_G}{1+\gamma} + V_{photo}$ under a fixed gate voltage V_G, which corresponds to the increase of the effective gate voltage V_G^{eff} given by the following equation:

$$V_G^{eff} = V_G + (1+\gamma)V_{photo} \quad (1)$$

So the offset gate voltage is given by: $V_{offset} = (1 + \gamma)V_{photo}$. Therefore, the shift of the transfer curve to a lower gate voltage under light irradiation can be explained.

According to our previous experience,[32] γ of the OPECT device can be characterized by changing the ion concentrations of aqueous solutions used in device measurements (Figure S1, Supporting Information). We can find that the transfer curve of the device measured in a KCl solution shifts for 186.9 mV when K^+ concentration is changed for one order of magnitude and thus the value of γ is estimated to be 2.16. Since the offset voltage V_{offset} shown in Figure 1c is about 550 mV, the photovoltage V_{photo} is calculated to be 174 mV for the device, according to Equation (1). It is obvious that V_{photo} is dependent on the photochemical property of the PEC gate. Therefore, a novel OPECT biosensor based on the variation of V_{photo} can be developed, in which biomolecules will be immobilized on the gate electrode to change the photochemical property.

Figure 2a shows the transient behavior (I_{DS} ~ time) of the OPECT under several repeated light on/off cycles measured at constant working voltages (V_G = 0 V, V_{DS} = 0.1 V). We can find that I_{DS} decreases under light irradiation, which is consistent with the shift of the transfer curve of the device shown in Figure 1c. The channel current response (I_{step}) at a light on/off cycle is given by the following equation:

$$I_{step} = I_{DS}^{off} - I_{DS}^{on} \quad (2)$$

where I_{DS}^{off} and I_{DS}^{on} correspond to channel currents when light is off and on, respectively. It is notable that the channel current response shows excellent repeatability at several light on/off cycles. Figure 2b shows time-dependent gate current (I_G) at several light on/off cycles, which is measured simultaneously with the channel current I_{DS} presented in Figure 2a. We can find that I_G increases under the light irradiation, which can be attributed to the electron transfer on the ITO gate electrode (Faradaic contribution).[34] For comparison, the same ITO electrode modified with CdS QDs was characterized under the same light irradiation in a traditional PEC bioanalysis (Figure S2, Supporting Information). It is reasonable to find that the gate current I_G is quite similar to the anodic photocurrent measured in the traditional PEC bioanalysis. Both currents show similar response at light on/off cycles with the magnitude of several μA. It is worth noting that the channel current response is at the order of several hundred μA, which is two orders of magnitude higher than the traditional PEC response. Furthermore, the

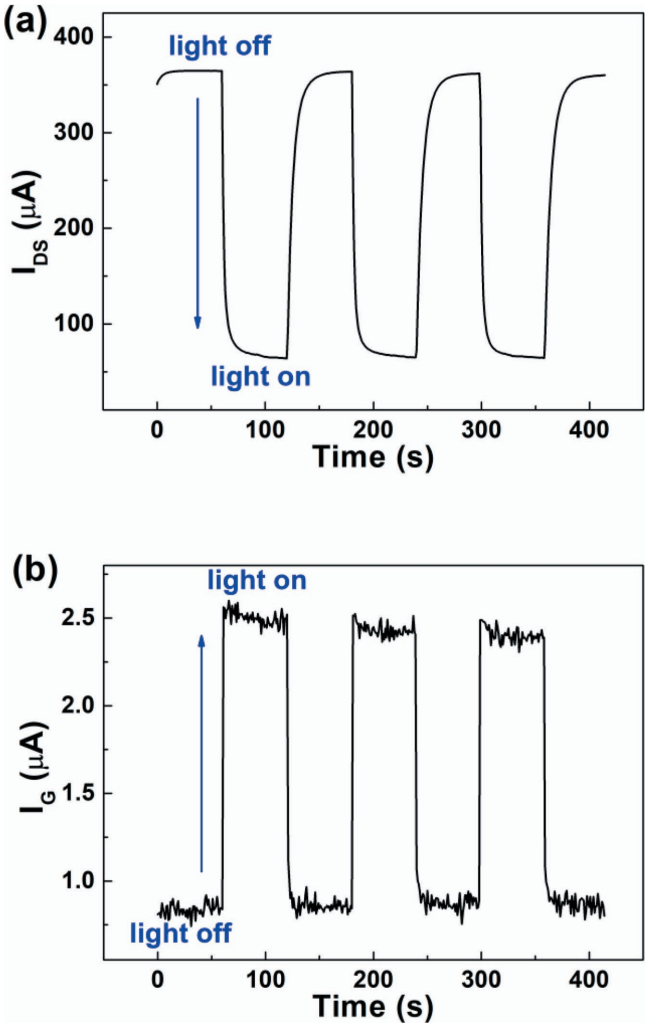

Figure 2. a) Channel current (I_{DS}) of an OPECT as a function of time (I_{DS} ~ time, V_G = 0 V, V_{DS} = 0.1 V) at several repeated light on/off cycles. b) The dependence of gate current (I_G) on time at several repeated light on/off cycles.

channel current I_{DS} in an OPECT can be further amplified if the width/length ratio of the transistor channel is increased, indicating that the device can serve as both an amplifier and a sensor.[35] Therefore, the OPECT-based biosensors are expected to be much more sensitive than conventional PEC bioanalysis.

The above experiments indicate that the charge transfer between the photosensitive semiconductor and the gate electrode plays an important role in the device performance of an OPECT-based sensor. To better understand the effect, another photosensitive semiconductor called Polymer dots (Pdots) was used in an OPECT for comparison, which was synthesized by the reprecipitation method using photosensitizer tetraphenylporphyrin (TPP) and a conjugated polymer poly[(9,9-dioctylfluorenyl-2,7-diyl)-co-(1,4-benzo-{2,1′,3}-thiadazole)] (PFBT). The TPP-doped PFBT Pdots showed a cathodic photocurrent in traditional PEC bioanalysis (Figure S3d, Supporting Information), which was reported in our previous work.[36] As shown in Figure S3a in the Supporting Information, electrons are transferred from the ITO electrode to TPP-doped PFBT

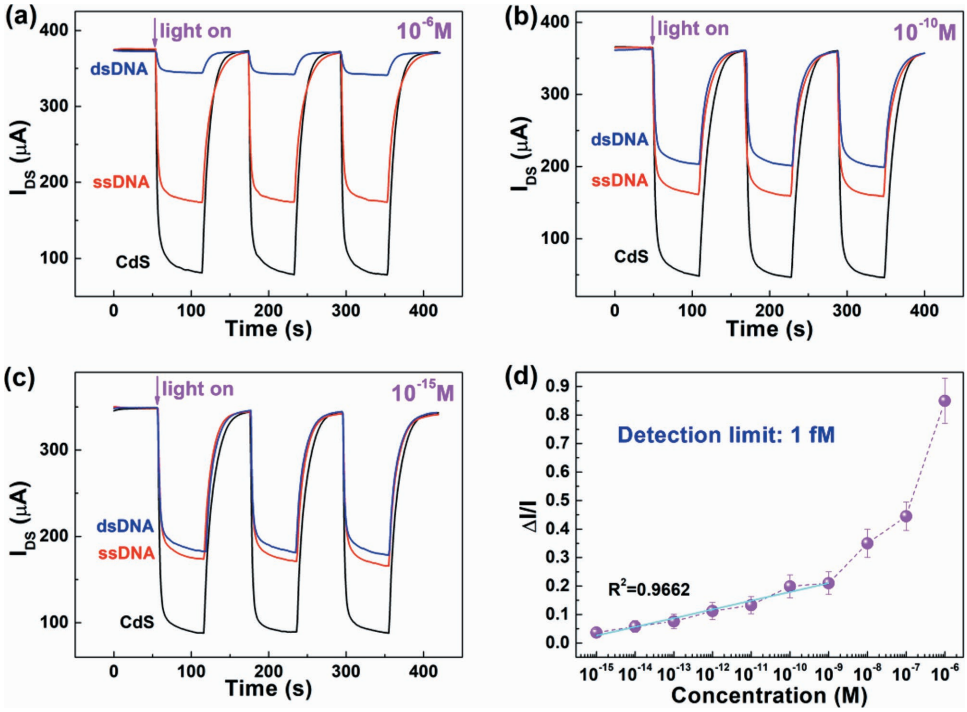

Figure 3. Channel current I_{DS} versus time (V_G = 0 V, V_{DS} = 0.1 V) at several repeated light on/off cycles for an OPECT device measured in three steps (Step 1: only CdS QDs, Step 2: immobilization of DNA, Step 3: hybridization of DNA). The concentration of the ssDNA probes is 1×10^{-6} M. The concentration of the ssDNA targets is: a) 1×10^{-6} M; b) 1×10^{-10} M; c) 1×10^{-15} M. d) $\Delta I/I$ as a function of the concentration of ssDNA targets. The detection limit of the OPECT-based DNA sensors is as low as 1×10^{-15} M. The linear relationship can be obtained from 1×10^{-15} to 1×10^{-9} M ($S = 0.4855 + 0.0306 \log C$, $R^2 = 0.9662$). Data are represented as mean ± SD, $n = 3$.

Pdots under the irradiation of 420 nm light, which is opposite to the charge transfer direction on an electrode of ITO/CdS QDs. As a result, the potential drop at the gate/electrolyte interface in the OPECT increases (formation of negative V_{photo}), leading to the decrease of the effective gate voltage V_G^{eff} and the shift of the transfer curve to a higher gate voltage (Figure S3b,c, Supporting Information). Therefore, the two charge transfer directions between the photosensitive semiconductor and the gate electrode under light irradiation, corresponding to anodic and cathodic photocurrent in traditional PEC bioanalysis, can lead to different responses (negative or positive shift of transfer curves) of OPECTs. We consider that both types of PEC electrodes can be used in OPECTs for sensing applications.

Next, a highly sensitive and selective DNA sensor based on OPECT has been investigated. Exciton–plasmon interactions (EPIs) have been widely studied in optoelectronic devices due to the interesting light-matter interplay between the exciton and plasmon.[37–39] The EPI effect designed in traditional PEC bioanalysis has been successfully utilized as a feasible approach for biodetection.[40–42] Therefore, an OPECT-based biosensor with the EPI effect between CdS QDs and Au nanoparticles (NPs) was developed for DNA sensing in our lab. As shown in Figure 1a, the ITO gate electrode was first modified with CdS QDs. Single-stranded DNA probes were then immobilized onto CdS QDs via the classic coupling reactions between the NH_2 groups on ssDNA probes and COOH groups on CdS QDs. Finally, the devices were used for the detection of complementary ssDNA targets labeled with Au NPs, which were prepared through the reactions of Au NPs with 5′-thiol-capped target DNA. The DNA sequences of 10 base pairs were used first, as shown in Table S1 in the Supporting Information. **Figure 3**a shows I_{DS} versus time (V_G = 0 V, V_{DS} = 0.1 V) at several repeated light on/off cycles for an OPECT device measured in three steps (Step 1: only CdS QDs, Step 2: immobilization of DNA, Step 3: hybridization of DNA). The concentrations of the ssDNA probes and targets are 1×10^{-6} M. It can be found that $I_{step}\left(I_{DS}^{off} - I_{DS}^{on}\right)$ decreases after the immobilization of ssDNA probes. After the hybridization of ssDNA probes with ssDNA targets, I_{step} is further decreased. Similar results can be obtained for the measurements of ssDNA targets with different concentrations of 1×10^{-15}–1×10^{-6} M, in which the concentration of ssDNA probes is fixed at 1×10^{-6} M, as shown in Figure 3b,c. Here we use $\Delta I/I$ to represent the signal response due to the hybridization of DNA, which is given by the following equation:

$$\frac{\Delta I}{I} = \frac{I_{step}^{ssDNA} - I_{step}^{dsDNA}}{I_{step}^{ssDNA}} \quad (3)$$

where I_{step}^{ssDNA} and I_{step}^{dsDNA} correspond to current responses (I_{step}) after the immobilization of ssDNA probes and the hybridization of ssDNA probes with ssDNA targets, respectively. Figure 3d shows the dependence of $\Delta I/I$ on the concentration of ssDNA targets. We can find that $\Delta I/I$ is decreased from 85% to 3.7% when the concentration of ssDNA targets is decreased from 1×10^{-6} to 1×10^{-15} M. As $\Delta I/I$ caused by pure PBS solution (baseline noise) is only 1%, the detection limit (signal response is three times higher than the baseline noise) of our

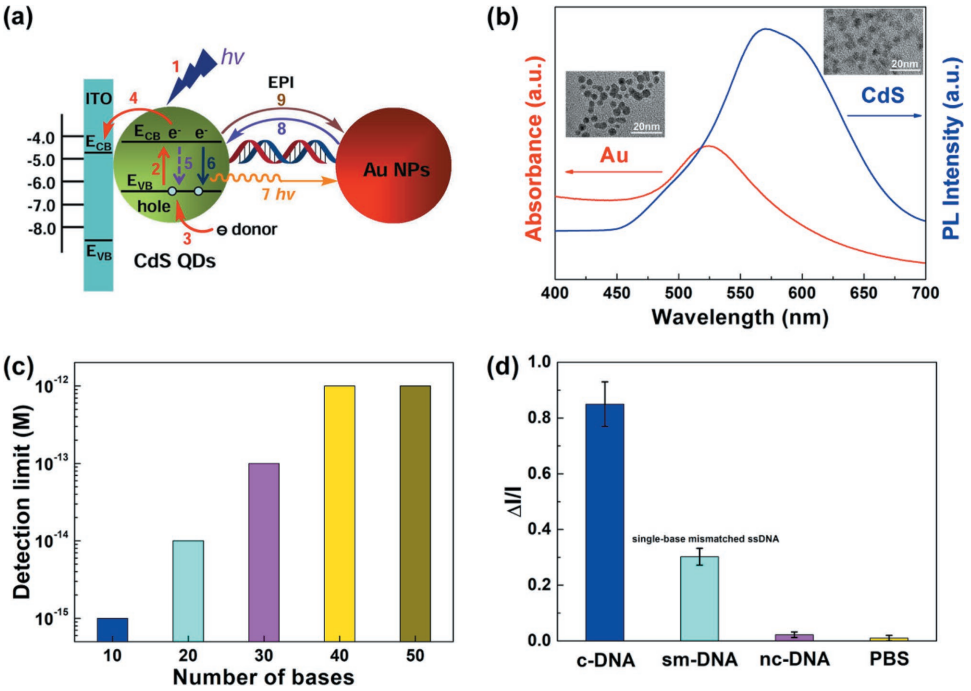

Figure 4. a) Schematic of the EPIs between CdS QDs and Au NPs on the gate electrode of an OPECT. b) The UV–vis absorption spectrum of prepared Au NPs and the PL spectrum of prepared CdS QDs. Insets are the TEM images of Au NPs (5 ± 1 nm) and CdS QDs (5 ± 1 nm), respectively. c) The detection limit of the OPECT-based DNA sensors for the detection of ssDNA targets with sequence of 10, 20, 30, 40, and 50 base pairs. d) The selectivity of the OPECT-based DNA sensor, which shows $\Delta I/I$ for the detection of complementary ssDNA targets, single-base mismatched ssDNA targets, noncomplementary ssDNA targets (10 base pairs, 1×10^{-6} M), and pure PBS solution. Data are represented as mean ± SD, $n = 3$.

OPECT-based DNA sensor can reach 1×10^{-15} M, which is one to two orders of magnitude better than that of traditional PEC bioanalysis (Figure S4, Supporting Information). Moreover, the detection limit of OPECT-based DNA sensor (1×10^{-15} M) is four orders of magnitude better than that of OECT-based DNA sensor (1×10^{-11} M) reported in our previous work.[10] A linear relationship can be obtained in the concentration region from 1×10^{-15} to 1×10^{-9} M. The linear regression equation is $S = 0.4855 + 0.0306 \log C$ (S is the signal response, C is the concentration of ssDNA targets, $R^2 = 0.9662$).

The sensing mechanism of the OPECT-based DNA sensor is studied. As shown in **Figure 4**a, the hybridization of ssDNA probes with Au NPs-labeled ssDNA targets can lead to the adjacence of Au NPs with CdS QDs. Our UV–vis absorption spectra clearly proved that Au NPs were well labeled in ssDNA targets, as shown in Figure S5 in the Supporting Information. Moreover, CdS QDs, ssDNA probes, and targets could be well modified on the ITO gate electrodes by some commonly used methods reported in our previous work (Experimental Section, Supporting Information).[40] So the EPI effect between CdS QDs and Au NPs can be the main reason for the signal change of the channel current of the OPECT device. To confirm it, ssDNA targets without Au NPs were also detected in control experiments. Figure S6a in the Supporting Information shows that $\Delta I/I$ is only 8.4% for the ssDNA targets without Au NPs (10 base pairs, 1×10^{-6} M), which is much lower than the value (85%) for Au NPs-labeled ssDNA targets. Meanwhile, the detection limit for the ssDNA targets without labeling is only 1×10^{-8} M.

Steric hindrance effect has been considered to be an important issue in traditional PEC bioanalysis.[43,44] Hence, electrochemical impedance spectroscopy (EIS) was used to characterize the ITO electrode with the three different modification states (only CdS QDs, immobilization of DNA, and hybridization of DNA, Figure S6b, Supporting Information). The concentrations of the ssDNA probes and targets are all 1×10^{-6} M. We can find that the impedance curve changes very little after the hybridization of DNA, which indicates that steric hindrance effect shows little influence on the sensing performance of our OPECT-based DNA sensors.

Therefore, Au NPs play an important role in the sensing performance of OPECT-based DNA sensors. As shown in Figure 4a, when the Au NPs-labeled ssDNA targets are hybridized with the ssDNA probes, the Au NPs are close to the CdS QDs. The irradiation of 420 nm light (process 1) on CdS QDs will lead to the excitation of electrons from the VB to the CB (process 2) and generate electron–hole pairs. The existence of strong electron donor AA (process 3) will then bring about the stable charge transfer from CdS QDs to ITO gate electrode (process 4), which results in the change of the potential drop (formation of photovoltage V_{photo}) at the gate/electrolyte interface. At the same time, the recombination (process 5 or 6) of electron–hole pairs occurs inevitably. The spontaneous emission of CdS QDs (process 7) caused by the radiative decay (process 6) will excite surface plasmon resonance (SPR) of the adjacent Au NPs, which creates local electric fields to enhance the radiative decay rate and thus the recombination of electron–hole pairs conversely (process 8).[45,46] Figure 4b shows the

typical UV–vis absorption spectrum of prepared Au NPs and the photoluminescence (PL) spectrum of prepared CdS QDs. It is worth noting that the spectra overlap between the absorption spectra of Au NPs and the emission spectra of CdS QDs is beneficial to efficient excitation of the SPR. On the other hand, the exciton energy transfer (EET) from CdS QDs to Au NPs (process 9) occurs simultaneously, accompanying with nonradiative decay (process 5) and thus another route for the recombination of electron–hole pairs.[47,48]

For the EPI effect between CdS QDs and Au NPs, both SPR and EET processes can enhance the recombination of electron–hole pairs and work together cooperatively. As a result, the EPI effect weakens the charge transfer from CdS QDs to ITO gate electrode (process 4), leading to the decrease of photovoltage V_{photo} in the OPECT device. Therefore, in Figure 3a, I_{step} decreases significantly after the hybridization of ssDNA probes with Au NPs-labeled ssDNA targets. It should be emphasized that the decrease of I_{step} after the immobilization of ssDNA probes could be mainly attributed to steric hindrance effect, because the long-time treatment (12 h) for the DNA immobilization may lead to the increase of surface impedance of the ITO electrode, which has been confirmed by EIS result (Figure S6b, Supporting Information).

It has been reported that the distance between the metal NPs and the semiconductor QDs is critical to the EPI effect.[49,50] To investigate this effect, DNA sequences of 10, 20, 30, 40, and 50 base pairs were then used to control interparticle distances. As the length of three base pairs is about 1 nm, the maximum interparticle distances for straight DNA chains are estimated to be 3–17 nm (Table S1, Supporting Information). We can find that the detection limit of DNA sensors becomes worse (from 1×10^{-15} to 1×10^{-12} M) with the increase of DNA length, as shown in Figure 4c. As EET is a short-range effect, the energy transfer could be reduced with the increasing interparticle distance.[51] In addition, SPR would be weakened as well when the interparticle distance increases because of lower absorption of Au NPs to the spontaneous emission of CdS QDs.[52] Therefore, the EPI effect between CdS QDs and Au NPs becomes weaker with the increase of DNA length, which leads to the decrease of the signal response and the sensitivity of the device. On the other hand, with the increase of the DNA length, the weight and volume of DNA increase. For the ssDNA targets without Au NPs, the detection limit of DNA sensors is improved from 1×10^{-8} to 1×10^{-11} M when the DNA sequences are increased from 10 to 50 base pairs (Figure S7, Supporting Information), which means that the steric hindrance effect is more pronounced for long DNAs. But even for the longest target DNA of 50 base pairs, the labeling of Au NPs can improve the detection limit for one order of magnitude, indicating that EPI effect is the major reason for the sensing performance.

It is worth noting that selectivity is also a very important parameter in evaluating the performance of a biosensor. For comparison, single-base mismatched ssDNA targets, noncomplementary ssDNA targets (10 base pairs, 1×10^{-6} M) and a pure PBS solution were used to modify the PEC gates. The responses ($\Delta I/I$) of the three devices are 30.2%, 2.2%, and 1%, respectively (Figure 4d and Figure S8, Supporting Information). The control experiments indicate the good selectivity of our OPECT-based DNA sensors.

In the field of DNA sensing, various detection techniques have been investigated, including dielectrophoretic, electrophoresis, colorimetric, fluorescence, and electrochemical impedance methods. Generally, the detection methods with optical readout have high sensitivity, in which the detection limit of 10^{-8}–10^{-16} M can be obtained.[53–55] However, optical methods usually need large equipment. For example, fluorescence quantitative polymerase chain reaction method can obtain ultralow detection limit of attomoles level due to the DNA replication technique,[56–58] but the measurements are time consuming and unportable. The detection methods based on electrochemical processes are more convenient and portable, which show the detection limit of about 10^{-8}–10^{-15} M.[59] Notably, the detection limit of the OPECT-based DNA sensor is as low as 10^{-15} M, indicating that OPECT is one of the best electrochemical biosensors for DNA detection. Although our OPECT-based DNA sensors need labeling, the labeling process is very convenient (Experimental Section, Supporting Information). More importantly, the detection limit reported in this work (10^{-15} M) is several orders of magnitude better than those of label-free detection methods based on organic devices (10^{-9}–10^{-13} M).[60,61] Normally, DNA microarrays use oligonucleotide probes with 10–25 nucleotides for the detection and analysis of functional genes and relative activities.[62,63] As the OPECT-based DNA sensors exhibit sensitive detection of DNA hybridization (10–20 base pairs), they are promising for applications in genetic mutations, genotyping, and microbial pathogens.[64,65] Based on the sensing platform of OPECTs, we will be able to develop many other ultrasensitive biosensors for the detection of various biomoleculars, especially those biomarkers with ultralow expression levels.[66]

In summary, we have exploited a new type of organic transistor OPECT and used it as a novel high-performance DNA sensor. The sensing mechanism of OPECTs is attributed to the photovoltage at the gate/electrolyte interface under light irradiation, which is induced by the charge transfer between the photosensitive semiconductor and the gate electrode. The DNA sensor based on OPECT exhibits very high sensitivity and selectivity. The detection limit of the DNA sensor can reach to 1×10^{-15} M, which is several orders of magnitude better than that of traditional PEC bioanalysis. As a new type of biosensor, OPECT is expected to be a promising platform for various biosensing applications, such as enzymatic sensors, immunosensors, cell-based biosensors, and so on. This work also provides a different technical perspective for the further development and implementation of organic bioelectronics.

Supporting Information

Supporting Information is available from the Wiley Online Library or from the author.

Acknowledgements

This work was financially supported by the National Natural Science Foundation of China (Nos. 61771318, 21675080), the Fundamental Research Project of Shenzhen (No. JCYJ20170302145633009), the Natural Science Foundation of SZU (No. 827-000022), the Natural

Science Foundation of Jiangsu Province (Grant BK20170073), and the Research Grants Council (RGC) of Hong Kong, China (Project No. C5015-15G).

Conflict of Interest

The authors declare no conflict of interest.

Keywords

DNA sensors, exciton–plasmon interaction, organic electrochemical transistors, organic photo-electrochemical transistors, photo-electrochemical sensors

Received: May 16, 2018
Revised: June 30, 2018
Published online:

[1] M. U. Ahmed, I. Saaem, P. C. Wu, A. S. Brown, *Crit. Rev. Biotechnol.* **2014**, *34*, 180.
[2] S. Kumar, W. Ahlawat, R. Kumar, N. Dilbaghi, *Biosens. Bioelectron.* **2015**, *70*, 498.
[3] E. B. Bahadır, M. K. Sezgintürk, *Anal. Biochem.* **2015**, *478*, 107.
[4] A. P. F. Turner, *Chem. Soc. Rev.* **2013**, *42*, 3184.
[5] L. Torsi, M. Magliulo, K. Manoli, G. Palazzo, *Chem. Soc. Rev.* **2013**, *42*, 8612.
[6] L. Kergoat, B. Piro, D. T. Simon, M. C. Pham, V. Noël, M. Berggren, *Adv. Mater.* **2014**, *26*, 5658.
[7] T. Someya, Z. Bao, G. G. Malliaras, *Nature* **2016**, *540*, 379.
[8] A. M. Pappa, V. F. Curto, M. Braendlein, X. Strakosas, M. J. Donahue, M. Fiocchi, G. G. Malliaras, R. M. Owens, *Adv. Healthcare Mater.* **2016**, *5*, 2295.
[9] C. Z. Liao, C. H. Mak, M. Zhang, H. L.W. Chan, F. Yan, *Adv. Mater.* **2015**, *27*, 676.
[10] P. Lin, X. T. Luo, I. M. Hsing, F. Yan, *Adv. Mater.* **2011**, *23*, 4035.
[11] D. J. Kim, N. E. Lee, J. S. Park, I. J. Park, J. G. Kim, H. J. Cho, *Biosens. Bioelectron.* **2010**, *25*, 2477.
[12] A. Williamson, M. Ferro, P. Leleux, E. Ismailova, A. Kaszas, T. Doublet, P. Quilichini, J. Rivnay, B. Rózsa, G. Katona, C. Bernard, G. G. Malliaras, *Adv. Mater.* **2015**, *27*, 4405.
[13] P. Lin, F. Yan, J. J. Yu, H. L.W. Chan, M. Yang, *Adv. Mater.* **2010**, *22*, 3655.
[14] C. Z. Liao, M. Zhang, M. Y. Yao, T. Hua, L. Li, F. Yan, *Adv. Mater.* **2015**, *27*, 7493.
[15] P. Lin, F. Yan, *Adv. Mater.* **2012**, *24*, 34.
[16] D. Khodagholy, J. Rivnay, M. Sessolo, M. Gurfinkel, P. Leleux, L. H. Jimison, E. Stavrinidou, T. Herve, S. Sanaur, R. M. Owens, G. G. Malliaras, *Nat. Commun.* **2013**, *4*, 2133.
[17] S. M. Zhang, E. Hubis, G. Tomasello, G. Soliveri, P. Kumar, F. Cicoira, *Chem. Mater.* **2017**, *29*, 3126.
[18] W. W. Zhao, J. J. Xu, H. Y. Chen, *Chem. Soc. Rev.* **2015**, *44*, 729.
[19] W. W. Zhao, J. J. Xu, H. Y. Chen, *Chem. Rev.* **2014**, *114*, 7421.
[20] H. Zhou, J. Liu, S. S. Zhang, *TrAC, Trends Anal. Chem.* **2015**, *67*, 56.
[21] A. Devadoss, P. Sudhagar, C. Terashima, K. Nakata, A. Fujishima, *J. Photochem. Photobiol., C* **2015**, *24*, 43.
[22] J. Tang, Y. Y. Zhang, B. Kong, Y. C. Wang, P. M. Da, J. Li, A. A. Elzatahry, D. Y. Zhao, X. G. Gong, G. F. Zheng, *Nano Lett.* **2014**, *14*, 2702.
[23] W. W. Zhan, Q. Kuang, J. Z. Zhou, X. J. Kong, Z. X. Xie, L. S. Zheng, *J. Am. Chem. Soc.* **2013**, *135*, 1926.
[24] J. Tanne, D. Schäfer, W. Khalid, W. J. Parak, F. Lisdat, *Anal. Chem.* **2011**, *83*, 7778.
[25] W. W. Zhao, S. Shan, Z. Y. Ma, L. N. Wan, J. J. Xu, H. Y. Chen, *Anal. Chem.* **2013**, *85*, 11686.
[26] Q. Kang, L. X. Yang, Y. F. Chen, S. L. Luo, L. F. Wen, Q. Y. Cai, S. Z. Yao, *Anal. Chem.* **2010**, *82*, 9749.
[27] W. W. Zhao, Z. Y. Ma, D. Y. Yan, J. J. Xu, H. Y. Chen, *Anal. Chem.* **2012**, *84*, 10518.
[28] Y. P. Wu, B. T. Zhang, L. H. Guo, *Anal. Chem.* **2013**, *85*, 6908.
[29] X. R. Zhang, Y. P. Xu, Y. Q. Zhao, W. L. Song, *Biosens. Bioelectron.* **2013**, *39*, 338.
[30] D. A. Bernards, D. J. Macaya, M. Nikolou, J. A. DeFranco, S. Takamatsu, G. G. Malliaras, *J. Mater. Chem.* **2008**, *18*, 116.
[31] H. J. Parab, C. Jung, J. H. Lee, H. G. Park, *Biosens. Bioelectron.* **2010**, *26*, 667.
[32] P. Lin, F. Yan, H. L. W. Chan, *ACS Appl. Mater. Interfaces* **2010**, *2*, 1637.
[33] D. A. Bernards, G. G. Malliaras, *Adv. Funct. Mater.* **2007**, *17*, 3538.
[34] G. Tarabella, C. Santato, S. Y. Yang, S. Iannotta, G. G. Malliaras, F. Cicoira, *Appl. Phys. Lett.* **2010**, *97*, 123304.
[35] F. Yan, H. Tang, *Expert Rev. Mol. Diagn.* **2010**, *10*, 547.
[36] Y. Li, N. Zhang, W. W. Zhao, D. C. Jiang, J. J. Xu, H. Y. Chen, *Anal. Chem.* **2017**, *89*, 4945.
[37] A. O. Govorov, G. W. Bryant, W. Zhang, T. Skeini, J. Lee, N. A. Kotov, J. M. Slocik, R. R. Naik, *Nano Lett.* **2006**, *6*, 984.
[38] J. Lee, P. Hernandez, J. Lee, A. O. Govorov, N. A. Kotov, *Nat. Mater.* **2007**, *6*, 291.
[39] E. Cohen-Hoshen, G. W. Bryant, I. Pinkas, J. Sperling, I. Bar-Joseph, *Nano Lett.* **2012**, *12*, 4260.
[40] W. W. Zhao, P. P. Yu, Y. Shan, J. Wang, J. J. Xu, H. Y. Chen, *Anal. Chem.* **2012**, *84*, 5892.
[41] W. W. Zhao, J. Wang, J. J. Xu, H. Y. Chen, *Chem. Commun.* **2011**, *47*, 10990.
[42] F. Xu, Y. C. Zhu, Z. Y. Ma, W. W. Zhao, J. J. Xu, H. Y. Chen, *Chem. Commun.* **2016**, *52*, 3034.
[43] N. Haddour, J. Chauvin, C. Gondran, S. Cosnier, *J. Am. Chem. Soc.* **2006**, *128*, 9693.
[44] W. W. Zhao, P. P. Yu, J. J. Xu, H. Y. Chen, *Electrochem. Commun.* **2011**, *13*, 495.
[45] M. Futamata, Y. Maruyama, M. Ishikawa, *J. Phys. Chem. B* **2003**, *107*, 7607.
[46] X. D. Hoa, A. G. Kirk, M. Tabrizian, *Biosens. Bioelectron.* **2007**, *23*, 151.
[47] M. Li, S. K. Cushing, Q. Y. Wang, X. D. Shi, L. A. Hornak, Z. L. Hong, N. Q. Wu, *J. Phys. Chem. Lett.* **2011**, *2*, 2125.
[48] Y. Shan, J. J. Xu, H. Y. Chen, *Chem. Commun.* **2009**, 905.
[49] M. M. Maye, O. Gang, M. Cotlet, *Chem. Commun.* **2010**, *46*, 6111.
[50] K. Matsuda, Y. Ito, Y. Kanemitsu, *Appl. Phys. Lett.* **2008**, *92*, 211911.
[51] O. Kulakovich, N. Strekal, A. Yaroshevich, S. Maskevich, S. Gaponenko, I. Nabiev, U. Woggon, M. Artemyev, *Nano Lett.* **2002**, *2*, 1449.
[52] L. He, E. A. Smith, M. J. Natan, C. D. Keating, *J. Phys. Chem. B* **2004**, *108*, 10973.
[53] X. D. Fan, I. M. White, S. I. Shopova, H. Y. Zhu, J. D. Suter, Y. Z. Sun, *Anal. Chim. Acta* **2008**, *620*, 8.
[54] S. Su, J. W. Fan, B. Xue, L. H. Yuwen, X. F. Liu, D. Pan, C. H. Fan, L. H. Wang, *ACS Appl. Mater. Interfaces* **2014**, *6*, 1152.
[55] M. Zhang, Y. M. Guan, B. C. Ye, *Chem. Commun.* **2011**, *47*, 3478.
[56] W. Ma, H. Kuang, L. G. Xu, L. Ding, C. L. Xu, L. B. Wang, N. A. Kotov, *Nat. Commun.* **2013**, *4*, 2689.
[57] M. Miedouge, M. Greze, A. Bailly, J. Izopet, *J. Clin. Virol.* **2011**, *50*, 57.
[58] L. Chang, D. M. Rissin, D. R. Fournier, T. Piech, P. P. Patel, D. H. Wilson, D. C. Duffy, *J. Immunol. Methods* **2012**, *378*, 102.
[59] E. G. Hvastkovs, D. A. Buttry, *Analyst* **2010**, *135*, 1817.

[60] S. Lai, M. Barbaro, A. Bonfiglio, *Sens. Actuators, B* **2016**, *233*, 314.
[61] H. U. Khan, M. E. Roberts, O. Johnson, R. Förch, W. Knoll, Z. Bao, *Adv. Mater.* **2010**, *22*, 4452.
[62] L. Bodrossy, A. Sessitsch, *Curr. Opin. Microbiol.* **2004**, *7*, 245.
[63] W. T. Liu, H. Guo, J. H. Wu, *Appl. Environ. Microbiol.* **2007**, *73*, 73.
[64] R. B. Stoughton, *Annu. Rev. Biochem.* **2005**, *74*, 53.
[65] E. S. Lander, *Nat. Genet.* **1999**, *21*, 3.
[66] Y. Fu, N. X. Wang, A. N. Yang, H. K.-W. Law, L. Li, F. Yan, *Adv. Mater.* **2017**, *29*, 1703787.